IEEE Access
Multidisciplinary ⋮ Rapid Review ⋮ Open Access Journal

Received 26 September 2023, accepted 28 September 2023, date of publication 4 October 2023,
date of current version 11 October 2023.

Digital Object Identifier 10.1109/ACCESS.2023.3321642

RESEARCH ARTICLE

Performance of Multi-RIS-Assisted D2D Communication Using NOMA

PRADEEP KUMAR, ABHIJIT BHOWMICK, AND YOGESH KUMAR CHOUKIKER, (Senior Member, IEEE)
Department of Communication Engineering, SENSE, Vellore Institute of Technology, Vellore, Tamil Nadu 632014, India
Corresponding author: Abhijit Bhowmick (abx.abhi99@gmail.com)

This work was supported by the Vellore Institute of Technology, Vellore, Tamil Nadu, India.

ABSTRACT Future 5G technologies increase spectrum efficiency and wireless capacity by supporting numerous connections at once. New designs are therefore required in order to support the future 5G vision. A desirable technique for beyond 5G, device-to-device (D2D) communication improves spectrum efficiency, capacity and lowers end-to-end latency as devices in close proximity interact directly with one another without using cellular infrastructure. As a result, the network needs a new, efficient D2D communication framework that can boost network performance. D2D communication with re-configurable intelligent surface (RIS) improves the performance of a communication network. In this work, a multi-RIS-assisted D2D communication using non-orthogonal multiple access (MRDN) network is studied. The proposed MRDN network model investigates the outage and throughput performance over Rician fading channels. Two possibilities are taken into consideration in this regard: (i) choosing the best received signal, and (ii) combining all received signals. Influence of imperfect successive interference cancellation (SIC) is explored to maintain practicability as NOMA is employed. In this regard, a thorough network modeling is carried out and new analytical formulas for the probability density function (PDF) of the equivalent channel and combined channel, outage, and throughput are developed. It is observed that combining of all received signals scenario performs better as compared to the other one. The impact of the number of RIS elements on the performance of the MRDN is significant. The performance of MRDN improves as the number of RIS increases. Performance of non-orthogonal multiple access (NOMA) scheme is also compared with the conventional orthogonal multiple access (OMA) scheme. Capacity gain is also investigated to test the superiority of NOMA over OMA.

INDEX TERMS D2D communication, MRDN, NOMA, throughput, RIS, outage.

I. INTRODUCTION

In recent years, the rapid increase in wireless devices as well as the enormous growth in data traffic have fueled the demand for more efficient and dependable communication technologies [1]. Device-to-device (D2D) communication can be one of the possible solutions to this problem, which allows direct communication between adjacent wireless devices without the need for a centralised network infrastructure [2]. On the other hand, D2D communication has technological challenges like interference management, resource allocation, mode selection, link selection, and relay selection [2], [3], [4] etc. Urban areas are becoming more crowded and denser due to rapid development and mass mobilisation. Beyond 5G, wireless communication networks are predicted to be ultra-dense due to the massive demand for wireless services. As a result, there is an exponential growth in both wireless users as well as obstacles to wireless signals. An inexpensive reconfigurable intelligent surface (RIS) has been studied to enhance coverage and serve all users adequately. In this context, reconfigurable intelligent surfaces (RISs) are emerging as a promising technology capable of dramatically improving network coverage and providing adequate coverage to all users [5]. Even a RIS

The associate editor coordinating the review of this manuscript and approving it for publication was Barbara Masini.

assisted network is helpful to reduce the effect of doppler shift and multipath fading effectively [6], [7]. The performance of D2D networks can be enhanced by integrating RIS into the network [8].

A RIS-assisted D2D network is helpful to establish connectivity between D2D devices when no direct path is available [9], [10], [11]. A RIS-assisted D2D communication network is studied over Rician fading channels in [10]. It is also observed that with an increment in the number of reflecting elements of RIS, there is an improvement in system performance in terms of outage probability, ergodic achievable rate, and average bit error rate [11], [12]. Authors studied the impact of hardware impairment on the proposed D2D network. They observed that the effect of hardware impairment can be mitigated with an increase in passive elements of RIS. In [13], a RIS assisted network is studied where multiple D2D users share the same cellular spectrum. The obtained results indicate that with deployment of RIS in the proposed D2D network, interference at the D2D receivers can be effectively reduced and it helps to achieve a much higher sum-rate in comparison to network without-RIS [13]. In [14], quality of service analysis is carried out for a RIS-assisted D2D communication network. The study considered both cases when the channel state information (CSI) is known at the transmitter and vice versa. Authors have observed that when CSI is not known, the packet drop ratio increases, so a hybrid automatic repeat request retransmission mechanism is applied to increase the throughput. The authors also observed that with an increase in the number of RIS elements, effective throughput can be improved up to five times.

The authors of [9], [10], [11], [12], and [13] proposed above works with Orthogonal Multiple Access (OMA). According to [15], the OMA is not sufficiently capable of managing and serving a huge number of users in a future communication network. On the other hand, many multiple-access techniques have been proposed while considering the future communication network, among which non-orthogonal multiple access (NOMA) is the most popular among researchers [15]. Good connection, low latency, and good spectral/energy efficiency are all capabilities of the NOMA. NOMA distributes non-orthogonal resources to numerous users, resulting in improved spectral efficiency, as opposed to orthogonal multiple access (OMA) systems that utilise orthogonal resources. Using only NOMA or RIS may not provide the full benefits of the technologies in many applications [16]. Integrating the RIS assisted network with the NOMA scheme can improve the system performance extensively [16]. The RIS-assisted NOMA network has much superior network performance than the OMA network [17]. The RIS-assisted NOMA network may have two possible ways of beamforming: each beam can serve multiple users at a time, or each beam can serve only one user [18]. In [19], the performance of near and far users is studied for the RIS-assisted OMA and NOMA networks while considering hardware impairments. Authors have found that system performance depends on the transmit power, power allocation factors, and number of RIS elements. According to [20], the RIS-assisted communication is better performer than a full-duplex relay based communication. In [21], the secrecy of outage probability is examined in the RIS-assisted NOMA network in the presence of eavesdroppers. The authors had observed that there was a negative impact from the increase in the number of RIS elements on secrecy performance, as eavesdroppers can also benefit from RIS. Moreover, secrecy performance can be enhanced by using group selection. The studies of the above-mentioned articles [17], [18], [19], [20], [21], clearly indicate that adopting the NOMA scheme in a RIS-assisted network can improve the network performance significantly.

D2D communication is also explored with RIS-assisted networks using the NOMA scheme to enhance the performance of a D2D network [22], [23], [24]. The authors of [23] and [24], observed enhancements in spectral and energy efficiency with the inclusion of the RIS and NOMA scheme in their proposed D2D network. Moreover, the authors of [24] proposed a hybrid-NOMA scheme that performs better in comparison to RIS-NOMA and RIS-OMA schemes over the proposed network. The effect of the RISE-6G project of European Union (EU), which is targeting the network of 2030 and beyond, inspired the researchers to explore the possibility of a multi-RIS-assisted communication network [25], [26].

Various multi-RIS-assisted networks are examined to enhance the performance of the different network scenarios [27], [28], [29], [30], [31], [32]. The proposed study of [27], indicates that there is a significant impact on network performance from the use of multiple RISs and the increase in the number of RIS elements. Multiple-RIS-assisted networks also help to improve energy efficiency and reduce the failure rate of D2D users [28]. In [29], multiple RIS-assisted D2D communication using the NOMA scheme is studied. Here, the authors examined a scenario where different groups of D2D users are assisted by multiple RIS to enhance the data rate of D2D groups. They have observed that system throughput can be enhanced by increasing the number of RIS in the network or by increasing the number of RIS reflecting elements. In [30], considering the situation of dense urban areas and large dense factries where the path of the single RIS itself is blocked, multiple RISs are assisting to extend the transmitted signal. The authors observed an enhancement in ergodic capacity with an increase in the number of RISs and RIS-reflecting elements. In [31], the authors present the different deployment scenarios of RIS-assisted communication networks to enhance the connectivity and reliability of the following wireless communication networks based on the suggestions of the ongoing EU RISE 6G project. The investigation of a NOMA-enabled D2D communications system with several RIS deployments to improve service quality for mobile D2D groups is found in [29]. A multi-agent multi-pass deep Q-network based framework is used to

optimize the sub-channel assignment, power allocation, and phase shifts adjustment policy of mobile D2D groups in order to maximize the average sum data rate [29]. Reference [32] examined the ergodic capacity and outage probability of the multi-RIS assisted multi-user NOMA system. Researchers found that the NOMA system with RISs performs much better in terms of outage probability and ergodic capacity. The active beamforming vectors, passive reflecting coefficients, and power splitting coefficients are jointly optimized in [33] to maximize the achievable information rate among all users while taking into account their minimum harvested energy needs and the transmitter's overall power budget.

A. MOTIVATION AND CONTRIBUTIONS

The above discussion motivates to explore the opportunities to develop an effective and robust communication network model that can match the expectations of future wireless communication. D2D communication lessens the base station's traffic burden, whereas NOMA offers service to several customers at once while using the same frequency resource and reducing interference with SIC, resulting in improved spectrum efficiency. A limited degree of control over channels is further provided via RIS integration. Thus, in this article, RIS-assisted D2D communication is investigated considering Rician fading channels, where D2D users are using the CU channel for their signal transmission using NOMA scheme. To improve the user experience, multiple RISs are placed in the considered network. The proposed multi-RIS-assisted D2D communication using NOMA (MRDN) network is examined for two different scenarios: selection of the best among the signals received via RISs and combining the received signals. New analytical frameworks for performance metrics have been developed. The primary contributions of this article are highlighted below:

- In this work, a MRDN network is proposed. Over Rician fading channels, the proposed network model is investigated.
- Both the dominant NLoS and LoS conditions are discussed and investigated for the proposed MRDN network.
- The proposed MRDN is examined over two scenarios: (i) Case-1: Selection of the best signals and (ii) Case-2: Combining of the received signals.
- New analytical expressions for the probability distribution functions of the equivalent and combined channels, outage, and network throughput are developed.
- Impact of degree of imperfection in SIC on the network performance is studied.
- Capacity gain of the proposed MRDN network model is also investigated.

B. ORGANIZATION OF THE PAPER

The paper is organized as follows: In Section II, network modeling and performance analysis of the proposed network model is discussed. Results and related discussions are presented in Section III and finally conclusion of the present study is presented in Section IV. In section IV, appendix is included where detail derivations are given. List of acronyms, symbols, and parameters value are given in Table. 1, Table. 2, and Table. 3.

TABLE 1. Acronyms.

Acronyms	Meaning
BS	Base station
CU	Cellular user
CSI	Channel state information
D2D	Device to Device
MRDN	multi-RIS-assisted D2D communication with NOMA
NLoS	Non Line of Sight
NOMA	Non-Orthogonal Multiple Access
OMA	Orthogonal Multiple Access
RIS	Reconfigurable Intelligent Surface
SIC	Successive interference cancellation
SNR/SINR	Signal-to-noise ratio/Signal-to-interference-plus-noise ratio

TABLE 2. Glossary of principal symbols.

Symbols	Meaning
$h_{Bi,k}$	Link among BS and the k_{th} pacth of RIS-i
$g_{1i,k}$	Link among k_{th} pacth of RIS-1 and D_i
$g_{2i,k}$	Link among k_{th} pacth of RIS-2 and D_i
D_i	i_{th} D2D user
$n_{11}/n_{12}/n_{21}/n_{22}$	AWGN noise
σ_n^2	Variance of the noise signal
$v_k^2/2\sigma_k^2$	Power in LoS/ NLoS component
λ_T/C_{th}	sensing/ censoring threshold
$\gamma_{D1,i}/\gamma_{D2,i}$	Received SNR at D_1 and D_2 through i_{th} RIS
$\gamma_{D1,C}/\gamma_{D2,C}$	Received SNR at D_1 and D_2 for $Case-2$
$P_{out,Di,S}$	Probability of outage at i_{th} D_i for $Case-1$
$P_{out,Di,C}$	Probability of outage at i_{th} D_i for $Case-2$
R_{D_i}/R_{TT}	Throughput for i_{th} D_i / Total system

II. SYSTEM MODEL

The system model for the proposed MRDN is shown in Fig. 1. In this proposed work, it is assumed that the direct paths between BS and D2D users (D_i) are blocked, thus, BS transmits the information signal via RISs to the D2D users (D_i where $i = 1, 2,$ and M). To improve the experience of D2D users, M RISs are considered in the proposed network and they are placed at different locations as shown in Fig. 1. In Fig. 1, $M = 2$, i.e., the MRDN network consists of two RISs (RIS-1 and RIS-2), they are identical and each consists of N reflecting patches. In the considered network model, the users D_1 and D_2 receive information through RISs using NOMA scheme and sharing the CU band.

Here, $h_{B1,k}$ and $h_{B2,k}$ represent the first hop links, i.e., the links between BS and the k_{th} patch of RIS-1 and RIS-2

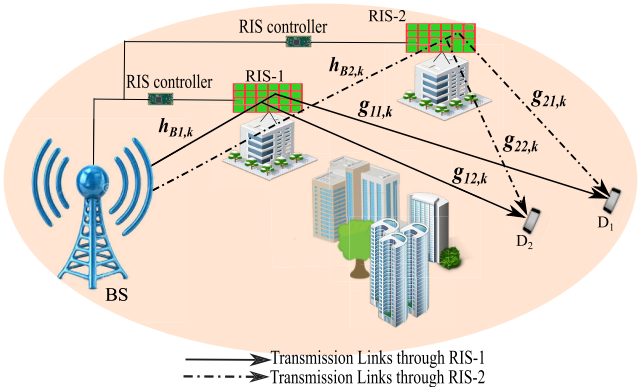

FIGURE 1. System model for transmission between BS and D2D users through RISs, $M = 2$.

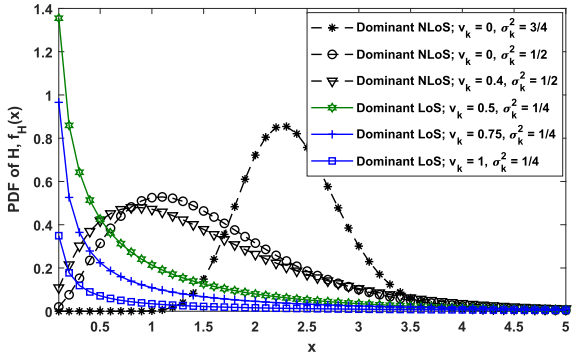

FIGURE 2. PDF of $f_H(x)$ for dominant NLoS and dominant LoS component.

respectively. Similarly, $g_{11,k}$ and $g_{12,k}$ represent the second hop links for D_1 and D_2 from RIS-1, i.e., the links between k_{th} patch of RIS-1 and D_1 and D_2 respectively. Similarly, $g_{21,k}$ and $g_{22,k}$ represent the second hop links for D_1 and D_2 from RIS-2, i.e., the links between k_{th} patch of RIS-2 and D_1 and D_2 respectively where $k = 1, 2, \ldots, N$. Channel vector for BS to RIS-1 is given by $h_{B1} = \left[h_{B1,1}, h_{B1,2}, \ldots, h_{B1,N}\right]^T$, for BS to RIS-2 is given by $h_{B2} = \left[h_{B2,1}, h_{B2,2}, \ldots, h_{B2,N}\right]^T$,and for RIS-$i$ to D_i is given by $g_{ii} = \left[g_{ii,1}, g_{ii,2}, \ldots, g_{ii,N}\right]^T$ where $i = 1, 2$. Here, all the first hop and second hop links are assumed to be Rician faded, independent and identically distributed (i.i.d.). The envelope of the channels in the first hop exist with shape parameter $K_{b,k}$ and scale parameter $\Omega_{b,k}$. Similarly, the envelope of the channels in the second hop exist with shape parameter $K_{ii,k}$ and scale parameter $\Omega_{ii,k}$. Let the power in line of sight (LoS) component is v_k^2 and the power in non-LoS (NLoS) component is $2\sigma_k^2$. Thus, the shape parameter and scale parameter can be described as $K_{b,k} = K_{ii,k} = \frac{v_k^2}{2\sigma_k^2}$, and $\Omega_{b,k} = \Omega_{ii,k} = v_k^2 + 2\sigma_k^2$.

A. CHANNEL MODEL

Each end-end link (BS to a D2D user) can be described by $H_{eq} = \sum_{k=1}^{N} H_k$ where $H_k = h_k g_k$ and H_{eq} is called equivalent channel coefficient. Since, h_k and g_k both are Rician faded, PDF of H_k can be expressed as [34],

$$f_{H_k}(x) = \sum_{j=1}^{\infty}\sum_{i=1}^{\infty} \frac{x^{i+j+1}\left(4K_{ii,k}^{i}K_{b,k}^{j}Z_1\right)Z_2}{(i!)^2(j!)^2 exp(K_{b,k}K_{ii,k})}, \tag{1}$$

where $Z_1 = \left(\Omega_{b,k}\Omega_{ii,k}\right)^{(i+j+2)/2}$, $Z_2 = K_{j-i}\left(2x\sqrt{\Omega_{b,k}\Omega_{ii,k}}\right)$, and $K_v(.)$ is the modified Bessel function of second kind and order v. Here, $|H| = \sum_{k=1}^{N} |H_k| = \sum_{k=1}^{N} |h_k||g_k|$. The mean value of h_k and g_k, i.e., $E[|h_k|]$ and $E[|g_k|]$ and their variance, i.e., $Var[|h_k|]$ and $var[|g_k|]$ are given by,

$$\begin{cases} E[|h_k|] = E[|g_k|] = \sqrt{\frac{\pi}{2}}\sigma_k L_{1/2}\left(-\frac{v_k^2}{2\sigma_k^2}\right), \\ Var[|h_k|] = Var[|g_k|] = 2\sigma_k^2 + v_k^2 - \frac{\pi}{2}\sigma_k^2\left[L_{1/2}\left(-\frac{v_k^2}{2\sigma_k^2}\right)\right]^2, \end{cases} \tag{2}$$

where $L_{1/2}(x) = exp(\frac{x}{2})\left[(1-x)I_0\left(-\frac{x}{2}\right) - xI_1\left(-\frac{x}{2}\right)\right]$, $I_v(.)$ is the v-th order modified Bessel function of first kind.

The PDF of H_{eq} can be written as [34],

$$f_{H_{eq}}(x) = \frac{x^a}{b^{a+1}\Gamma(a+1)} exp\left(-\frac{x}{b}\right), \tag{3}$$

where $a = \frac{(E[H_{eq}])^2}{Var[H_{eq}]} - 1$ and $b = \frac{Var[H_{eq}]}{E[H_{eq}]}$. The PDF of H_{eq}, i.e., $f_{H_{eq}}(x)$ for dominant NLoS and LoS conditions is shown in Fig.2. The impact of a number of RIS elements on the distribution is also shown in Fig. 3.

Proposition 1: A randomly distributed equivalent channel coefficient is a multiplication of two channel coefficients which follow Rician distribution. The mean and variance of the randomly distributed equivalent channel coefficient (H) are expressed as,

$$\begin{cases} E[|H_{eq}|] = \frac{N\pi}{2}\sigma_k^2\left[L_{1/2}\left(-\frac{v_k^2}{2\sigma_k^2}\right)\right]^2 \\ Var[|H_{eq}|] = N\left[2\sigma_k^2 - \frac{\pi^2}{4}\sigma_k^4\left\{L_{1/2}\left(-\frac{v_k^2}{2\sigma_k^2}\right)\right\}^4\right] + Nv_k^2. \end{cases} \tag{4}$$

Proof: Detail derivation is given in Appendix A.

Now, the $E[|H_{eq}|]$ and $Var[|H_{eq}|]$ of H_{eq} are evaluated for two conditions: (i) Dominant NLoS and (ii) Dominant LoS (refer to (5) and (6)).

1) DOMINANT NLoS

When NLoS is dominant, $\sigma_k^2 > v_k$. The analytical expression of the mean and variance of H, i.e., $E[|H_{eq}|]$ and $Var[|H_{eq}|]$,

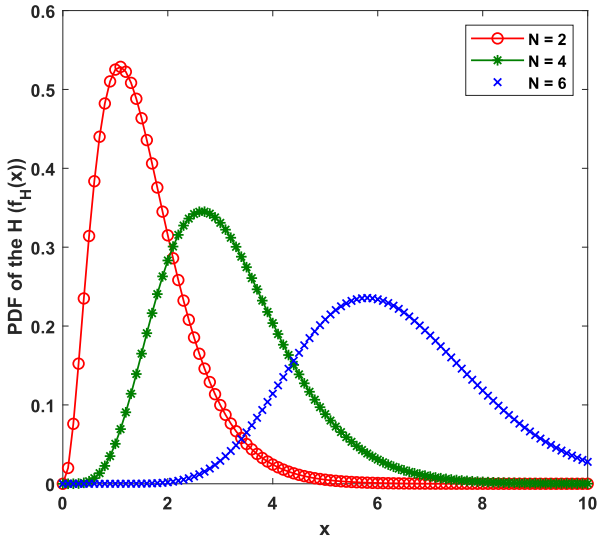

FIGURE 3. Impact of a number of RIS elements (N) on PDF of $f_H(x)$ for dominant NLoS component.

is evaluated for $v_k = 0$ and $\sigma_k^2 = \frac{1}{2}$. Thus,$E[|H_{eq}|]$ and $Var[|H_{eq}|]$ can be written as

$$\begin{cases} E[|H_{eq}|] = \dfrac{N\pi}{4}, \\ Var[|H_{eq}|] = N\left(1 - \dfrac{\pi^2}{16}\right). \end{cases} \tag{5}$$

2) DOMINANT LoS

When LoS is dominant, $v_k > \sigma_k^2$. For an example, while $v_k = 1$ and $\sigma_k^2 = \frac{1}{4}$, the LoS component becomes dominant. Hence,$E[|H_{eq}|]$ and $Var[|H_{eq}|]$ can be written as

$$\begin{cases} E[|H_{eq}|] = \dfrac{0.445\,N\pi}{8}, \\ Var[|H_{eq}|] = N\left(\dfrac{1}{2} - \dfrac{0.1979\pi^2}{64}\right) + N. \end{cases} \tag{6}$$

B. SIGNAL MODEL FOR DUAL RIS-ASSISTED COMMUNICATION

The BS transmits a superimposed signal of x_1 and x_2 to both the D2D users via RIS-1 and RIS-2 which is given by [35]

$$s_{bs} = \sqrt{\varphi_1 P}x_1 + \sqrt{\varphi_2 P}x_2, \tag{7}$$

where x_1 is for D_1 and x_2 is for D_2, P is the transmit power of BS, φ_1 and φ_2 are the power allocation coefficients for x_1 and x_2; and $\varphi_1 > \varphi_2$ with the criterion that $\varphi_1 + \varphi_2 = 1$. Power allocation is done on the basis of channel condition. The signal associated with good channel is allocated low power and vice versa. For an example, if $|H_i|^2 < |H_j|^2$, then $\varphi_i > \varphi_j$ where H_i and H_j are the channel coefficients associated with the i-th and j-th users. The received signals at D_1 through RIS-1 and RIS-2 are given by

$$y_{D1,1} = \sum_{k=1}^{N} h_{B1,k}\beta e^{j\phi_{k1}} g_{11,k}\left(\sqrt{\varphi_1 P}x_1 + \sqrt{\varphi_2 P}x_2\right) + n_{11}, \tag{8}$$

$$y_{D1,2} = \sum_{k=1}^{N} h_{B2,k}\beta e^{j\phi_{k2}} g_{21,k}\left(\sqrt{\varphi_1 P}x_1 + \sqrt{\varphi_2 P}x_2\right) + n_{12}, \tag{9}$$

where $h_{(.,k)} = \left|h_{(.,k)}\right| e^{-j\theta_k^u}$, $g_{(.,k)} = \left|g_{(.,k)}\right| e^{-j\theta_k^d}$ (here θ_k^u and θ_k^d are the angles for up-link and down-link channels for k-th element); n_{11} represents the sum of additive white Gaussian noise (AWGN) for the link from BS to D_1 via RIS-1, n_{12} represents the sum of AWGN for the link from BS to D_1 via RIS-2, β is the RIS reflection loss, $\phi_{k(.)}$ denotes the phase introduced at RIS, and $\sigma_{n_{11}}^2 = \sigma_{n_{12}}^2 = \sigma_n^2$. It is considered that there is no reflection loss, i.e., $\beta = 1$ and the RIS controller controls the phase introduced at RIS in a way that it cancels out the total phase introductions in the up-link and down-link ($\phi_{(.)} - \theta_k^u - \theta_k^d = 0$).

Hence, the received signal-to-interference-plus-noise ratios (SINRs) at D_1 (signals received through RIS-1 and RIS-2) can be expressed as,

$$\gamma_{D1,1} = \frac{\varphi_1 P\left|H_{eq,11}\right|^2}{\sigma_n^2 + \varphi_2 P\left|H_{eq,11}\right|^2}, \tag{10}$$

$$\gamma_{D1,2} = \frac{\varphi_1 P\left|H_{eq,12}\right|^2}{\sigma_n^2 + \varphi_2 P\left|H_{eq,12}\right|^2}, \tag{11}$$

where, $H_{eq,11} = \left|\sum_{k=1}^{N} h_{B1,k}\beta e^{j\phi_{k1}} g_{11,k}\right| = \sum_{k=1}^{N} |h_{B1,k}||g_{11,k}|$ and $H_{eq,12} = \left|\sum_{k=1}^{N} h_{B2,k}\beta e^{j\phi_{k2}} g_{21,k}\right| = \sum_{k=1}^{N} |h_{B2,k}||g_{21,k}|$ as $\beta = 1$ and $|e^{j\phi_{(.)}}| = 1$.

Similarly, the received signals at D_2 through RIS-1 and RIS-2 are given by

$$y_{D2,1} = \sum_{k=1}^{N} h_{B1,k}\beta e^{j\phi_{k1}} g_{12,k}\left(\sqrt{\varphi_1 P}x_1 + \sqrt{\varphi_2 P}x_2\right) + n_{21}, \tag{12}$$

$$y_{D2,2} = \sum_{k=1}^{N} h_{B2,k}\beta e^{j\phi_{k2}} g_{22,k}\left(\sqrt{\varphi_1 P}x_1 + \sqrt{\varphi_2 P}x_2\right) + n_{22}, \tag{13}$$

where n_{21} represents the sum of additive white Gaussian noise (AWGN) for the link from BS to D_2 via RIS-1, n_{22} represents the sum of AWGN for the link from BS to D_2 via RIS-2. For simplicity, it is also considered that $\sigma_{n_{21}}^2 = \sigma_{n_{22}}^2 = \sigma_n^2$ where σ_n^2 is the total noise power. The SINR for decoding of information of D_1 at D_2 is given by,

$$\gamma_{D2,1} = \frac{\varphi_1 P\left|H_{eq,21}\right|^2}{\sigma_n^2 + \varphi_2 P\left|H_{eq,21}\right|^2}, \tag{14}$$

$$\gamma_{D2,2} = \frac{\varphi_1 P\left|H_{eq,22}\right|^2}{\sigma_n^2 + \varphi_2 P\left|H_{eq,22}\right|^2}, \tag{15}$$

where $\gamma_{D2,1}$ is the received SINR at D_2 (due to communication through RIS-1) and $\gamma_{D2,2}$ is the received SINR (due to communication through RIS-2); $H_{eq,21} = \left|\sum_{k=1}^{N} h_{B1,k}\beta e^{j\phi_{k1}} g_{12,k}\right| = \sum_{k=1}^{N} |h_{B1,k}||g_{12,k}|$, and $H_{eq,22} = \left|\sum_{k=1}^{N} h_{B2,k}\beta e^{j\phi_{k2}} g_{22,k}\right| = \sum_{k=1}^{N} |h_{B2,k}||g_{22,k}|$. After perfect successive interference cancellation (SIC) the received signals at D_2 can be expressed as,

$$y_{D2,1} = H_{eq,21}\sqrt{\varphi_2 P}x_2 + n_{21}, \tag{16}$$

$$y_{D2,2} = H_{eq,22}\sqrt{\varphi_2 P}x_2 + n_{22}. \tag{17}$$

If the SIC is imperfect, then the received signals can be expressed as,

$$y_{D2,1} = H_{eq,21}\left[\sqrt{\xi\varphi_1 P}x_1 + \sqrt{\varphi_2 P}x_2\right] + n_{21}, \tag{18}$$

$$y_{D2,2} = H_{eq,22}\left[\sqrt{\xi\varphi_1 P}x_1 + \sqrt{\varphi_2 P}x_2\right] + n_{22}, \tag{19}$$

where $\xi\varphi_1 P|H_{(.)}|^2$ is residual SIC and ξ is the SIC inefficiency factor and its range is [0, 1]. Hence, the SNRs/SINRs for perfect and imperfect SIC at D_2 (signals received through RIS-1 and RIS-2) can be expressed as,

$$\gamma_{D2,1} = \begin{cases} \dfrac{\varphi_2 P|H_{eq,21}|^2}{\sigma_n^2}, & \text{Perfect SIC} \\ \dfrac{\varphi_2 P|H_{eq,21}|^2}{\sigma_n^2 + \xi\varphi_1 P|H_{eq,21}|^2}, & \text{Imperfect SIC} \end{cases} \tag{20}$$

$$\gamma_{D2,2} = \begin{cases} \dfrac{\varphi_2 P|H_{eq,22}|^2}{\sigma_n^2}, & \text{Perfect SIC} \\ \dfrac{\varphi_2 P|H_{eq,22}|^2}{\sigma_n^2 + \xi\varphi_1 P|H_{eq,22}|^2}, & \text{Imperfect SIC} \end{cases} \tag{21}$$

In this regards, two cases are considered:
(i) Case-1: Selection of best received signal.
(ii) Case-2: Combining of all received signals.
In Case-1, each D2D user selects the best between two received signals and in Case-2, each D2D user combines both the received signals.

C. CASE-1: SELECTION OF BEST RECEIVED SIGNAL

In this section, outage probability is evaluated for Case-1 scheme. It can be achieved by selecting the maximum received SNR/SINR. Thus, the selected SNR/SINR at D_1 and D_2 can be expressed as,

$$\gamma_{D1,S} = \max\left(\gamma_{D1,1}, \gamma_{D1,2}\right), \tag{22}$$

$$\gamma_{D2,S} = \max\left(\gamma_{D2,1}, \gamma_{D2,2}\right). \tag{23}$$

1) OUTAGE PROBABILITY

A D2D user suffers from outage while its receive SNR/SINR falls below a threshold SNR.

Proposition 2: When the channels of a D2D network are Rician faded, end-end communication is supported by dual-RISs and the D2D system follows the case-1, the closed form expressions for outage for D2D users (D_1 and D_2) can be described by the expressions given in (27) and (29).

Probability of outage at D_1 and D_2 occurs when the received SNR/SINR falls bellow a outage threshold (γ_{th}). The probability of outage at D_1 can be expressed as

$$\begin{aligned} P_{out,D1,S} &= P\left(\gamma_{D1,S} \le \gamma_{th}\right) \\ &= P\left(\max\left(\gamma_{D1,1}, \gamma_{D1,2}\right) \le \gamma_{th}\right) \\ &= P\left(\gamma_{D1,1} \le \gamma_{th}\right) P\left(\gamma_{D1,2} \le \gamma_{th}\right) \\ &= P\left(\frac{C_1|H_{eq,11}|^2}{1 + C_2|H_{eq,11}|^2} \le \gamma_{th}\right) \\ &\quad \times P\left(\frac{C_1|H_{eq,12}|^2}{1 + C_2|H_{eq,12}|^2} \le \gamma_{th}\right), \end{aligned} \tag{24}$$

where $C_1 = \varphi_1 P/\sigma_n^2$, and $C_2 = \varphi_2 P/\sigma_n^2$. Here, both $H_{eq,11}$ and $H_{eq,12}$ follow the distribution of H_{eq}. Now the aim is to find the $Z = P\left(\frac{C_1|H_{eq}|^2}{1+C_2|H_{eq}|^2} \le \gamma_{th}\right)$. After doing some algebra (24) reduces to

$$\begin{aligned} Z &= P\left(\frac{C_1|H_{eq}|^2}{1 + C_2|H_{eq}|^2} \le \gamma_{th}\right) \\ &= P\left(|H_{eq}| \le \gamma_{th1}\right) \\ &= \int_0^{\bar{\gamma}_{th1}} f_{H_{eq}}(x)dx, \end{aligned} \tag{25}$$

where $\bar{\gamma}_{th1} = \sqrt{\frac{\gamma_{th}}{C_1 - C_2\gamma_{th}}}$. The PDF $f_{H_{eq}}(x)$ given in (3) using in (25), after some algebra and using [36], Z reduces to

$$\begin{aligned} Z &= \frac{1}{b^{a+1}\Gamma(a+1)}\left[\frac{a!}{(1/b)^{a+1}}\right. \\ &\quad \left. -exp(-\bar{\gamma}_{th1})\sum_{k=0}^{a}\frac{a!\bar{\gamma}_{th1}^k}{k!(1/b)^{a-k+1}}\right] \\ &= \frac{1}{b^{a+1}\Gamma(a+1)}(1/b)^{-a-1}\gamma\left(a+1, \frac{\bar{\gamma}_{th1}}{b}\right), \end{aligned} \tag{26}$$

Hence, from (24), $P_{out,D1,S}$ can be expressed as,

$$\begin{aligned} P_{out,D1,S} &= Z \times Z \\ &= \left[\frac{1}{b^{a+1}\Gamma(a+1)}(1/b)^{-a-1}\gamma\left(a+1, \frac{\bar{\gamma}_{th1}}{b}\right)\right]^2, \end{aligned} \tag{27}$$

The detail derivation of (26) is shown in Appendix-B. The probability of outage at D_2 can be expressed as

$$\begin{aligned} P_{out,D2,S} &= P\left(\gamma_{D2,S} \le \gamma_{th}\right) \\ &= P\left(\max\left(\gamma_{D2,1}\gamma_{D2,2}\right) \le \gamma_{th}\right) \\ &= P\left(\gamma_{D2,1} \le \gamma_{th}\right) P\left(\gamma_{D2,2} \le \gamma_{th}\right) \end{aligned} \tag{28}$$

Both $H_{eq,3}$ and $H_{eq,4}$ follow the distribution of H_{eq}. Using the same process as done in (25)-(27) and after doing some

algebra, (28) reduces to

$$P_{out,D2,S} = \begin{cases} \left[\frac{(1/b)^{-a-1}}{b^{a+1}\Gamma(a+1)}\gamma\left(a+1,\frac{\bar{\gamma}_{th2}}{b}\right)\right]^2, & \text{Perfect SIC} \\ \left[\frac{(1/b)^{-a-1}}{b^{a+1}\Gamma(a+1)}\gamma\left(a+1,\frac{\bar{\gamma}_{th3}}{b}\right)\right]^2, & \text{Imperfect SIC} \end{cases} \tag{29}$$

where $\bar{\gamma}_{th2} = \frac{\gamma_{th}}{C_2}$, $\bar{\gamma}_{th3} = \sqrt{\frac{\gamma_{th}}{C_2 - C_3\gamma_{th}}}$, and $C_3 = \frac{\xi\varphi_1 P}{\sigma_n^2}$.

D. CASE-2: COMBINING OF ALL RECEIVED SIGNALS

In Case-2 scheme, the signals received at D_1 and D_2 from RIS-1 and RIS-2 are combined. Hence, the combined received signal at D_1 is given by,

$$\begin{aligned} y_{D1} &= y_{D1,1} + y_{D1,2} \\ &= \left(H_{eq,11} + H_{eq,12}\right)\left(\sqrt{\varphi_1 P}x_1 + \sqrt{\varphi_2 P}x_2\right) + n_{c,12}, \end{aligned} \tag{30}$$

where $n_{c,12} = (n_{11} + n_{21})$. Similarly, the combined received signal at D_2 is given by,

$$\begin{aligned} y_{D2} &= y_{D2,1} + y_{D2,2} \\ &= \left(H_{eq,21} + H_{eq,22}\right)\left(\sqrt{\varphi_1 P}x_1 + \sqrt{\varphi_2 P}x_2\right) + n_{c,22}, \end{aligned} \tag{31}$$

where $n_{c,22} = (n_{21} + n_{22})$. For simplicity, it is considered that $\sigma^2_{n_{c,12}} = \sigma^2_{n_{c,22}} = \sigma_n^2$.
The received SINR at D_1 and D_2 can be written as,

$$\gamma_{D1,C} = \frac{\varphi_1 P|H_{d1}|^2}{\sigma_n^2 + \varphi_2 P|H_{d1}|^2}, \tag{32}$$

$$\gamma_{D2,C} = \begin{cases} \frac{\varphi_2 P|H_{d2}|^2}{\sigma_n^2}, & \text{Perfect SIC} \\ \frac{\varphi_2 P|H_{d2}|^2}{\sigma_n^2 + \xi\varphi_1 P|H_{d2}|^2}, & \text{Imperfect SIC} \end{cases} \tag{33}$$

where $H_{d1} = \left(H_{eq,11} + H_{eq,12}\right)$ and $H_{d2} = \left(H_{eq,21} + H_{eq,22}\right)$.

Proposition 3: The PDF of combined channels (H_{ij}) can be expressed by the distribution indicated in (34) where $H_{ij} = H_i + H_j$.

$$f_{H_{ij}}(x) = \frac{exp\left(-\frac{x}{b}\right)}{\left[b^{a+1}\Gamma(a+1)\right]^2}x^{2a+1}B\left(a+1,a+1\right), \tag{34}$$

where $B(.,.)$ is the Beta function, $B\left(p,q\right) = \int_0^1 t^{p-1}(1-t)^{q-1}dt$.

Proof: See in Appendix C.

The PDF of combined channels H_{d1} and H_{d2} follow the PDF of H_{ij} which is shown in Fig.4.

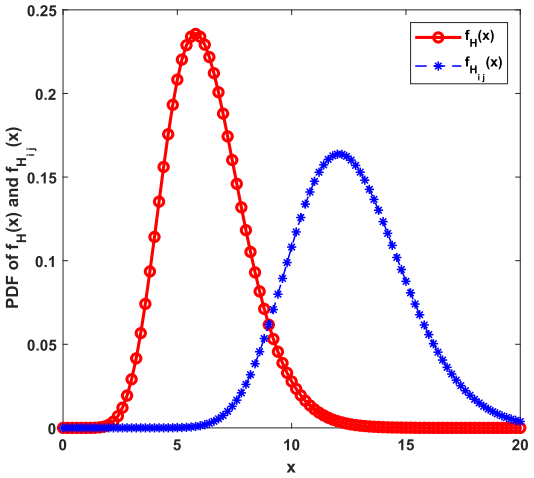

FIGURE 4. PDF of $f_{H_{ij}}(x)$ and $f_H(x)$ for dominant NLoS.

1) OUTAGE PROBABILITY

In this section the outage for each D2D user for case-2 is evaluated.

Proposition 4: The closed form expressions of outage at D_1 and D_2 for combining of the received signals from RIS-1 and RIS-2 are given in (38).

Hence, the outage for both the users can be described as,

$$\begin{aligned} P_{out,D1,C} &= P\left(\gamma_{D1,C} \le \gamma_{th}\right) \\ &= P\left(\frac{\varphi_1 P|H_{d1}|^2}{\sigma_n^2 + \varphi_2 P|H_{d1}|^2} \le \gamma_{th}\right) \\ &= P\left(\frac{C_1|H_{d1}|^2}{1 + C_2|H_{d1}|^2} \le \gamma_{th}\right), \end{aligned} \tag{35}$$

$$P_{out,D2,C} = P\left(\gamma_{D2,C} \le \gamma_{th}\right). \tag{36}$$

Hence, for perfect and imperfect SIC, (36) can be written as,

$$P_{out,D2,C} = \begin{cases} P\left(\frac{\varphi_2 P|H_{d2}|^2}{\sigma_n^2} \le \gamma_{th}\right), & \text{Perfect SIC} \\ P\left(\frac{\varphi_2 P|H_{d2}|^2}{\sigma_n^2 + \xi\varphi_1 P|H_{d2}|^2} \le \gamma_{th}\right), & \text{Imperfect SIC.} \end{cases} \tag{37}$$

After substitution and reduction (see Appendix D), $P_{out,D1,C}$ and $P_{out,D2,C}$ can be expressed as,

$$P_{out,D1,C} = \frac{B(a+1,a+1)}{[b^{a+1}\Gamma(a+1)]^2}(1/b)^{-2a-2}\gamma\left(2a+2,\frac{\bar{\gamma}_{th1}}{b}\right), \tag{38}$$

$$P_{out,D2,C} = \begin{cases} \frac{B(a+1,a+1)}{[b^{a+1}\Gamma(a+1)]^2}(1/b)^{-2a-2}\gamma\left(2a+2,\frac{\bar{\gamma}_{th2}}{b}\right), \\ \text{SIC}_\text{P} \\ \frac{B(a+1,a+1)}{[b^{a+1}\Gamma(a+1)]^2}(1/b)^{-2a-2}\gamma\left(2a+2,\frac{\bar{\gamma}_{th3}}{b}\right), \\ \text{SIC}_\text{IP}. \end{cases} \tag{39}$$

In (39), SIC_P indicates perfect SIC and SIC_{IP} indicates imperfect SIC. The SNR thresholds $\bar{\gamma}_{th1}$, $\bar{\gamma}_{th2}$ and $\bar{\gamma}_{th3}$ are outage thresholds and defined in the previous discussions.

Proof: See in Appendix D.

2) THROUGHPUT

D2D users share the CU channel for their transmission of information. Thus, the throughput for D_1 and D_2 for both cases are given by,

$$R_{D1,NOMA} = \begin{cases} \left(1 - P_{out,D1,S}\right) \log_2\left(1 + \gamma_{D1,S}\right), & \text{Case-1} \\ \left(1 - P_{out,D1,C}\right) \log_2\left(1 + \gamma_{D1,C}\right), & \text{Case-2} \end{cases} \tag{40}$$

$$R_{D2,NOMA} = \begin{cases} \left(1 - P_{out,D2,S}\right) \log_2\left(1 + \gamma_{D2,S}\right), & \text{Case-1} \\ \left(1 - P_{out,D2,C}\right) \log_2\left(1 + \gamma_{D2,C}\right), & \text{Case-2.} \end{cases} \tag{41}$$

Hence, the total throughput of D2D system is given by

$$R_{TT,NOMA} = R_{D1,NOMA} + R_{D2,NOMA}. \tag{42}$$

3) CAPACITY GAIN

Capacity gain is defined as the difference between the capacity for NOMA scheme and capacity for orthogonal multiple access (OMA) scheme.

$$C_{gain} = R_{TT,NOMA} - R_{TT,OMA}, \tag{43}$$

where $R_{TT,OMA}$ is the throughput for OMA scheme. In this sub-section, C_{gain} is studied for case-2. Here, $R_{TT,NOMA}$ for case-2 can be expressed as,

$$\begin{aligned} R_{TT,NOMA} &= \left(1 - P_{out,D1,C}\right) \log_2\left(1 + \gamma_{D1,C}\right) \\ &\quad + \left(1 - P_{out,D2,C}\right) \log_2\left(1 + \gamma_{D2,C}\right), \end{aligned} \tag{44}$$

$$\begin{aligned} R_{TT,OMA} &= \left(1 - \bar{P}_{out,C}\right) \left[\frac{1}{2} \log_2\left(1 + \bar{\gamma}_{D1,C}\right)\right. \\ &\quad \left. + \frac{1}{2} \log_2\left(1 + \bar{\gamma}_{D2,C}\right)\right]. \end{aligned} \tag{45}$$

In (45), link capacity for each user is expressed by $\frac{1}{2}\log_2(.)$. There are two users and the transmission time is divided between them. Thus, $\frac{1}{2}$ is multiplied with $\log_2(.)$ term. The received SNRs ($\bar{\gamma}_{D1,C}$ and $\bar{\gamma}_{D2,C}$) and outage ($\bar{P}_{out,C}$) are as follows:

$$\bar{\gamma}_{D1,C} = \frac{P|H_{d1}|^2}{\sigma_n^2}, \tag{46}$$

$$\bar{\gamma}_{D2,C} = \frac{P|H_{d2}|^2}{\sigma_n^2}, \tag{47}$$

$$\bar{P}_{out,C} = \frac{B(a+1,a+1)}{[b^{a+1}\Gamma(a+1)]^2}(1/b)^{-2a-2}\gamma\left(2a+2, \frac{\bar{\gamma}_{th4}}{b}\right), \tag{48}$$

and $\bar{\gamma}_{th4} = \sqrt{\frac{\gamma_{th}\sigma_n^2}{P}}$.

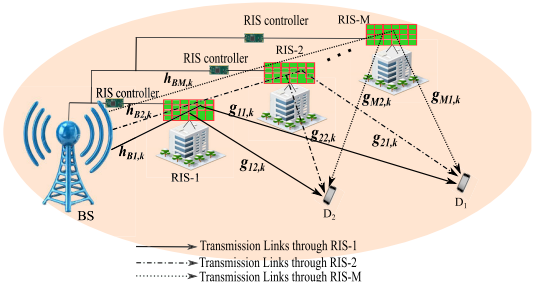

FIGURE 5. System model for muti-RIS scenario, $M > 2$.

E. SIGNAL MODEL FOR MULTI-RIS-ASSISTED COMMUNICATION

In this section, the performance is studied for Multi-RIS-assisted communication for Case-2 scenario (Fig. 5). It is considered that there are M number of RISs and they are assisting in communication between BS and D2D users. The received signal at D_1 can be expressed as,

$$\begin{aligned} y_{D1} &= y_{D1,1} + y_{D1,2} + \ldots + y_{D1,M} \\ &= \sum_{i=1}^{M} H_{eq,1i}\left(\sqrt{\varphi_1 P}x_1 + \sqrt{\varphi_2 P}x_2\right) + n_1 \\ &= \left(H_{eq,11} + H_{eq,12} + \ldots + H_{eq,1M}\right) \\ &\quad \times \left(\sqrt{\varphi_1 P}x_1 + \sqrt{\varphi_2 P}x_2\right) + n_1, \end{aligned} \tag{49}$$

Similarly, the received signal at D_2 can be written as,

$$\begin{aligned} y_{D2} &= y_{D2,1} + y_{D2,2} + \ldots + y_{D2,M} \\ &= \sum_{i=1}^{M} H_{eq,2i}\left(\sqrt{\varphi_1 P}x_1 + \sqrt{\varphi_2 P}x_2\right) + n_2 \\ &= \left(H_{eq,21} + H_{eq,22} + \ldots + H_{eq,2M}\right) \\ &\quad \times \left(\sqrt{\varphi_1 P}x_1 + \sqrt{\varphi_2 P}x_2\right) + n_2, \end{aligned} \tag{50}$$

where n_1 and n_2 are sum of additive white Gaussian noises received at D_1 and D_2 with variances σ_1^2 and σ_2^2 where $\sigma_1^2 = \sigma_2^2 = \sigma_n^2$. The received SINR at D_1 and D_2 can be written as,

$$\gamma_{D1,M} = \frac{\varphi_1 P|H_{m1}|^2}{\sigma_n^2 + \varphi_2 P|H_{m1}|^2} \tag{51}$$

$$\gamma_{D2,M} = \begin{cases} \dfrac{\varphi_2 P|H_{m2}|^2}{\sigma_n^2}, & \text{Perfect SIC} \\ \dfrac{\varphi_2 P|H_{m2}|^2}{\sigma_n^2 + \xi\varphi_1 P|H_{m2}|^2}, & \text{Imperfect SIC} \end{cases} \tag{52}$$

where $H_{m1} = \left(H_{eq,11} + H_{eq,12} + \ldots + H_{eq,1M}\right)$ and $H_{m2} = \left(H_{eq,21} + H_{eq,22} + \ldots + H_{eq,2M}\right)$. Hence, the outage for both the users for multi-RIS-assisted communication can be written as,

$$P_{out,D1,M} = P\left(\gamma_{D1,M} \leq \gamma_{th}\right), \tag{53}$$

$$P_{out,D2,M} = P\left(\gamma_{D2,M} \leq \gamma_{th}\right). \tag{54}$$

TABLE 3. Value of the parameters.

Parameters	Values
φ_1	0.8
φ_2	0.2
P	1 mW
σ_n^2	-80 dBm
v_k	0, 0.4, 0.5, 1
σ_k^2	1/4, 1/2, 1/8
N	2 to 10
ξ	0.01, 0.02, 0.04

Hence, for perfect and imperfect SIC, (54) can be written as,

$$P_{out,D2,M} = \begin{cases} P\left(\dfrac{\varphi_2 P|H_{m2}|^2}{\sigma_n^2} \le \gamma_{th}\right), & \text{Perfect SIC} \\ P\left(\dfrac{\varphi_2 P|H_{m2}|^2}{\sigma_n^2 + \xi\varphi_1 P|H_{m2}|^2} \le \gamma_{th}\right), & \text{Imperfect SIC} \end{cases} \tag{55}$$

Hence, the network throughput for D_1 and D_2, i.e., $R_{D1,M}$ and $R_{D2,M}$ and total throughput for multi-RIS scenario ($R_{TT,M}$) can be expressed as,

$$R_{D1,M} = \left(1 - P_{out,D1,M}\right)\log_2\left(1 + \gamma_{D1,M}\right), \tag{56}$$

$$R_{D2,M} = \left(1 - P_{out,D2,M}\right)\log_2\left(1 + \gamma_{D2,M}\right), \tag{57}$$

$$R_{TM,NOMA} = R_{D1,M} + R_{D2,M}. \tag{58}$$

F. PRACTICAL IMPLICATIONS OF THE PROPOSED WORK

The long-term evolution advanced (LTE-A) standard from the third generation partnership project (3GPP) is based on NOMA, also known as multiuser superposition transmission (MUST). More specifically, NOMA adoption enables simultaneous sharing of a subcarrier between many users in OFDMA without altering LTE resource blocks [37].

Social apps generally employ local services. Local service, emergency communication, and IoT improvement are examples of 5G D2D applications. User data is transferred directly between terminals and does not go through the network while using a local service. This would result in increased receiver complexity at the expense of improving spectrum efficiency.

III. RESULTS

Results and discussions are presented in this section based on the analytical modeling of the MRDN. The MATLAB platform is used to evaluate the performance of the D2D network scenario under consideration. The performance is investigated in terms of outage, throughput, and capacity gain. The network parameters and their values are used in this study are given in Table 3.

The outage performance of the D2D users is studied for Case-1 scheme for dominant LoS condition in Fig. 6. The performance is investigated for $v_k = 0.5$, $\sigma_k^2 = 1/4$, $\xi = 0.01$ and $N = 4$. It is observed that the outage increases as the outage threshold increases (γ_{th}). For a given outage threshold, outage at user D_1 is low as compared to user D_2.

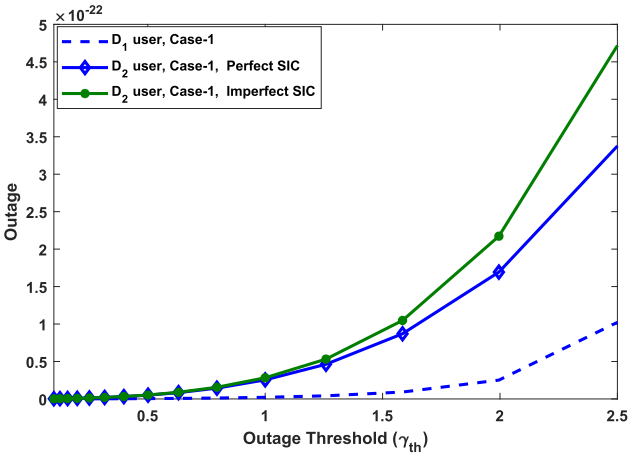

FIGURE 6. Outage vs outage threshold for D_1 and D_2 for dominant LoS (Case-1).

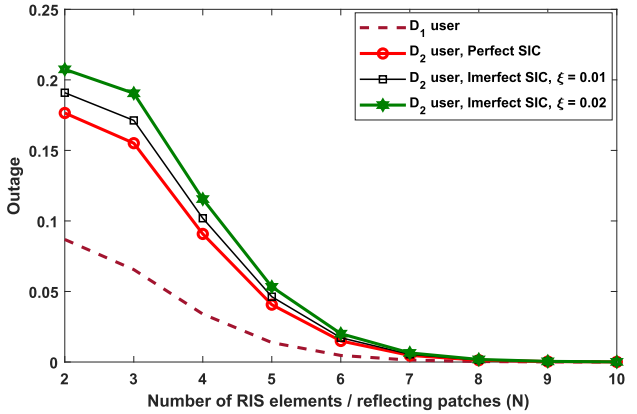

FIGURE 7. Outage vs number of RIS elements/patches for D_1 and D_2 for dominant LoS (Case-1).

It is also found that if the SIC is not perfect (user D_2), outage increases.

In Fig. 7, the outage performance investigated for dominant LoS for Case-1 scheme. The value of the parameters are considered as $v_k = 0.4$, $\sigma_k^2 = 1/8$, $\gamma_{th} = 2$, and $\xi = 0.01, 0.02$. It is observed that the outage for both users decreases as the number of RIS elements/ patches (N) increases. It is found that SIC inefficiency factor (ξ) has significant impact on the outage performance. For a given N, the outage increases as the ξ increases from 0.01 to 0.02.

In Fig. 8, outage is investigated for Case-1 and Case-2 schemes. The performance is studied for $v_k = 0.5$, $\sigma_k^2 = 1/4$, $\xi = 0.01$ and $N = 4$. It is found that for a given γ_{th}, compared to Case-1, Case-2 scheme has low outage. In Fig. 9, the impact of number of RIS patches on outage is studied for both Case-1 and Case-2 schemes. As the number of RIS patches increases, outage decreases. It is also observed that the outage increases as the imperfection in SIC increases.

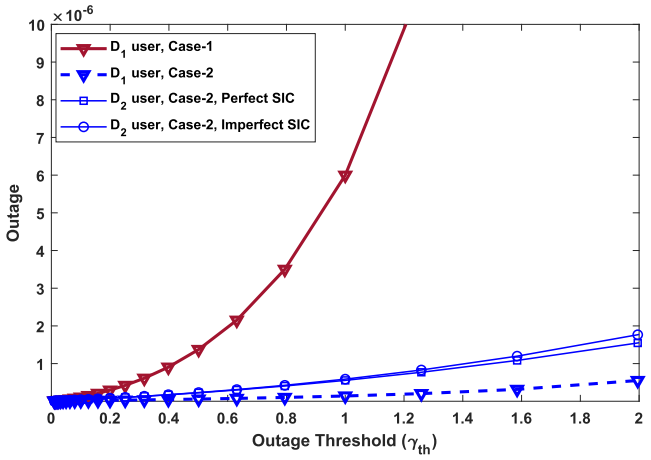

FIGURE 8. Outage for Case-1 and Case-2.

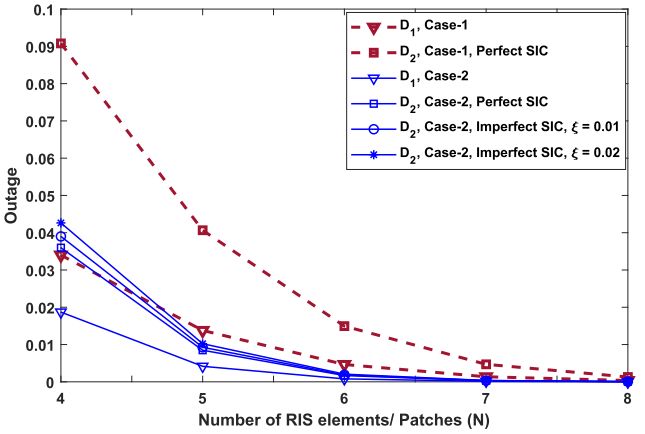

FIGURE 9. Outage vs number of RIS patches for Case-1 and Case-2.

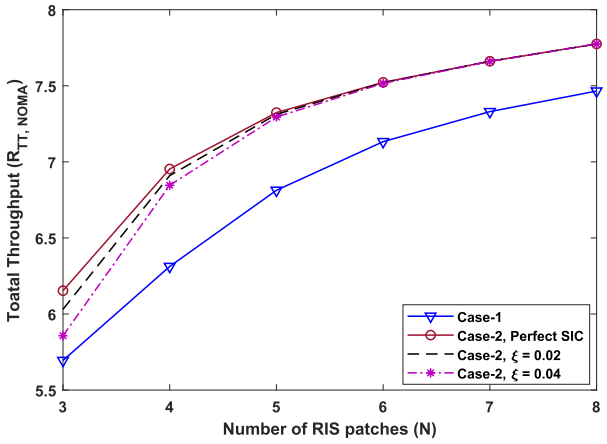

FIGURE 10. Impact of a number of RISs on total throughput for Case-1 with dominant LoS.

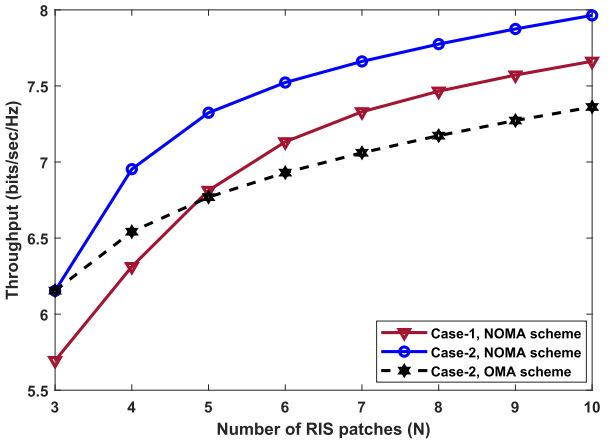

FIGURE 11. Comparative study for NOMA and OMA schemes.

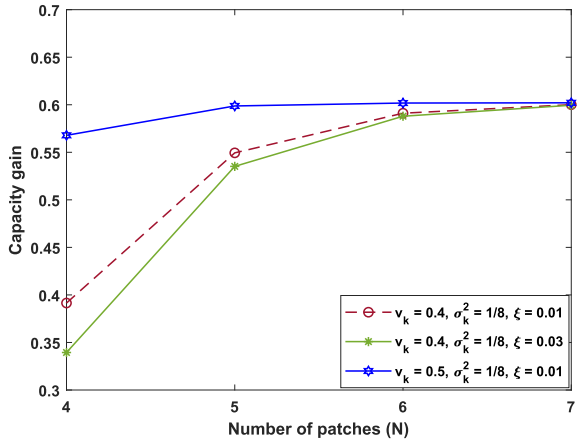

FIGURE 12. Capacity gain vs. Number of patches.

In Fig. 10, total throughput ($R_{TT,NOMA}$) performance is investigated for Case-1 and Case-2 schemes. The performance is studied for $v_k = 0.4$, $\sigma_k^2 = 1/8$, $\gamma_{th} = 2$, and $\xi = 0.01, 0.2$. It is found that the $R_{TT,NOMA}$ increases as the N increases. It also observed that for a particular number of RIS patches, total throughput decreases as the imperfection of SIC increases. Throughput for the Case-2 scheme outperforms the Case-1 scheme. In Fig. 11, throughput performance is compared for NOMA and OMA schemes. It is found that incorporation of NOMA scheme instead of OMA schemes improves the network performance significantly. Capacity gain is studied in Fig. 12. It is found that capacity gain increases as the number of patches in a RIS increases. It reduces as the imperfection in SIC (ξ) increases. On contrary, the capacity gain increases as the power in the LoS component increases.

In Fig. 13, total throughput performance ($R_{TM,NOMA}$) for multiple number of RISs, i.e., $M \geq 2$ is investigated for Case-2 scenario. The performance is studied for $v_k = 0.4$, $\sigma_k^2 = 1/8$, $\gamma_{th} = 2$, and $M = 2, 3, 4$. It is found that the total throughput increases as the N increases. It also observed that for a particular value of N, network throughput improves as the number of RISs, i.e., M increases. Impact of transmit power on throughput is studied in Fig. 14, It is observed that network throughput improves as the transmit power increases. It is also found that the

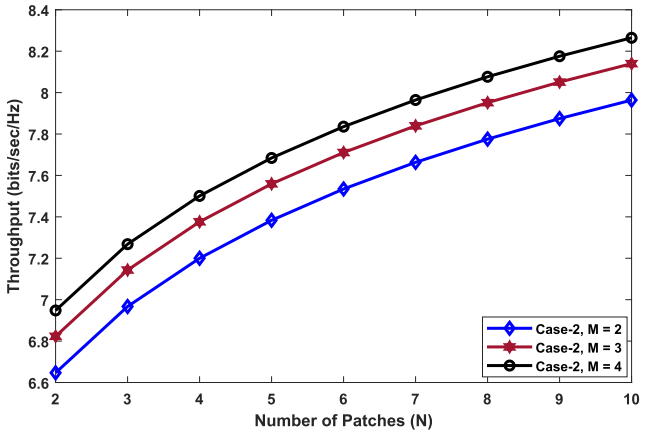

FIGURE 13. Throughput ($R_{TM,NOMA}$) vs. number of patches for multiple number of RISs (M).

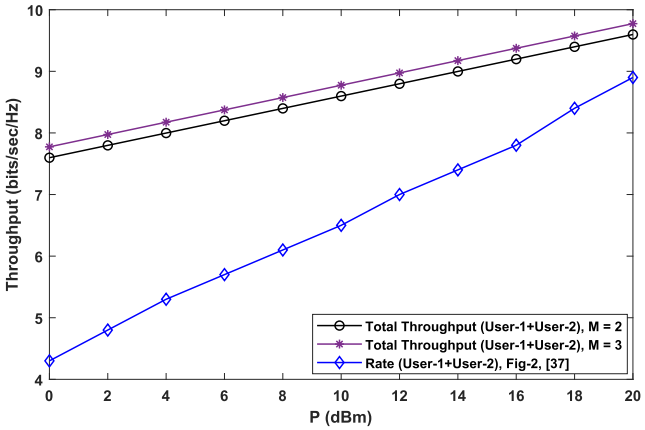

FIGURE 14. Impact of transmit power (P) on throughput ($R_{TM,NOMA}$).

throughput for proposed work outperforms the existing one.

IV. CONCLUSION

In this paper multi-RIS-assisted D2D communication using NOMA (MRDN) is studied. It is considered that the channels are Rician faded. Two conditions, i.e., dominant non-line of sight (NLoS) and dominant LoS are considered for performance investigation. Performance of the considered network is investigated under two scenarios: (i) selection of best, (ii) Combining of best and worst. In selection, a user selects the best one among the received signals while in the second scenario, user combines the best and worst received signals. The network performance is studied in terms of outage, throughput and capacity gain. In the first part, MRDN is studied with $M = 2$. Analytical expressions of PDF of equivalent channel and combined channel, outage, and throughput are developed. It is observed that Case-2 scheme performs better as compared to the Case-1 scheme. The number of RIS elements patches has significant impact on the performance of the MRDN. Increase in degree of imperfection in SIC technique degrades the network performance. The performance of NOMA and OMA is compared and observed NOMA is better as compared to the OMA. The capacity gain improves as the number of patches in a RIS increases. Later the study is extended for $M > 2$ scenario and observed that the network throughput improves significantly as M increases.

APPENDIXES

APPENDIX A

Here, $H = \sum_{k=1}^{N} H_k = \sum_{k=1}^{N} h_k g_k$. Therefore,

$$|H| = \sum_{k=1}^{N} |h_k||g_k|. \tag{59}$$

The mean values of h_k and g_k can be defined as $E[|h_k|] = E[|g_k|] = \sqrt{\frac{\pi}{2}}\sigma_k L_{1/2}\left(-\frac{v_k^2}{2\sigma_k^2}\right)$ and $Var[|h_k|] = Var[|g_k|] = 2\sigma_k^2 + v_k^2 - \frac{\pi}{2}\sigma_k^2\left[L_{1/2}\left(-\frac{v_k^2}{2\sigma_k^2}\right)\right]^2$ where $L_{1/2}(x) = exp(\frac{x}{2})\left[(1-x)I_0\left(-\frac{x}{2}\right) - xI_1\left(-\frac{x}{2}\right)\right]$, $I_v(.)$ is the v-th order modified Bessel function of the first kind. Thus, $E[|H|]$ can be written as,

$$\begin{aligned} E[|H|] &= \sum_{k=1}^{N} E[|h_k|]E[|g_k|] \\ &= \sum_{k=1}^{N}\left[\sqrt{\frac{\pi}{2}}\sigma_k L_{1/2}\left(-\frac{v_k^2}{2\sigma_k^2}\right)\right]\left[\sqrt{\frac{\pi}{2}}\sigma_k \right. \\ &\quad \left. \times L_{1/2}\left(-\frac{v_k^2}{2\sigma_k^2}\right)\right] \\ &= \frac{N\pi}{2}\sigma_k^2\left[L_{1/2}\left(-\frac{v_k^2}{2\sigma_k^2}\right)\right]^2. \end{aligned} \tag{60}$$

Now, the aim is to evaluate $Var[|H|]$ where $Var[|H|] = E[|H|^2] - [E[|H|]]^2$. First $E[|H|^2]$ and other related parameters is evaluated thereafter $Var[|H|]$ is evaluated.

$$\begin{aligned} E[|H|^2] &= E\left[(N^2-N)|h_i||g_i||h_j||g_j| + N|h_i|^2|g_i|^2\right] \\ &= (N^2-N)E[|h_i|]E[|g_i|]E[|h_j|]E[|g_j|] \\ &\quad + NE[|h_i|^2]E[|g_i|^2], \end{aligned} \tag{61}$$

where $E[|h_i|^2]] = E[|g_i|^2]]$; $E[|h_i|^2]]$ and $E[|g_i|^2]]$ can be expressed as,

$$\begin{aligned} E[|h_i|^2]] &= Var[|h_i|] + [E[|h_i|]]^2 \\ &= 2\sigma_k^2 + v_k^2 - \frac{\pi}{2}\sigma_k^2\left[L_{1/2}\left(-\frac{v_k^2}{2\sigma_k^2}\right)\right]^2 \\ &\quad + \frac{\pi}{2}\sigma_k^2\left[L_{1/2}\left(-\frac{v_k^2}{2\sigma_k^2}\right)\right]^2 \\ &= 2\sigma_k^2 + v_k^2. \end{aligned} \tag{62}$$

Therefore, after Using (60) and (62) in (61), $E[|H|^2]$ can be written as,

$$\begin{aligned} E[|H|^2] &= (N^2-N)E[|h_i|]E[|g_i|]E[|h_j|]E[|g_j|] \\ &\quad + NE[|h_i|^2]E[|g_i|^2] \\ &= (N^2-N)\frac{\pi^2}{4}\sigma_k^4\left[L_{1/2}\left(-\frac{v_k^2}{2\sigma_k^2}\right)\right]^4 \\ &\quad + N\left(2\sigma_k^2+v_k^2\right)^2, \end{aligned} \tag{63}$$

substituting $E[|H|^2]$ and $E[|H|]$ in the expression of $Var[|H|]$, $Var[|H|]$ can be expressed as,

$$\begin{aligned} Var[|H|] &= E[|H|^2] - [E[|H|]]^2 \\ &= N\left[2\sigma_k^2 - \frac{\pi^2}{4}\sigma_k^4\left\{L_{1/2}\left(-\frac{v_k^2}{2\sigma_k^2}\right)\right\}^4\right] \\ &\quad + Nv_k^2. \end{aligned} \tag{64}$$

(i) **Dominant NLoS:** When NLoS is dominant, $\sigma_k^2 > v_k$. To find the $E[|H|]$ and $Var[|H|]$, it is considered that $v_k = 0$ and $\sigma_k^2 = \frac{1}{2}$. Substituting the values of v_k and σ_k^2 in the expression of $E[|h_k|]$ and $Var[|h_k|]$, the mean values of h_k and g_k can be defined as $E[|h_k|] = E[|g_k|] = \sqrt{\frac{\pi}{4}}$ and $Var[|h_k|] = Var[|g_k|] = \frac{4-\pi}{4}$. Thus, $E[|H|]$ can be written as,

$$\begin{aligned} E[|H|] &= \frac{N\pi}{2}\sigma_k^2\left[L_{1/2}\left(-\frac{v_k^2}{2\sigma_k^2}\right)\right]^2 \\ &= \frac{N\pi}{2}\frac{1}{2}\left[L_{1/2}(0)\right]^2 \\ &= \frac{N\pi}{4}, \end{aligned} \tag{65}$$

where $L_{1/2}(x) = exp(\frac{x}{2})\left[(1-x)I_0\left(-\frac{x}{2}\right) - xI_1\left(-\frac{x}{2}\right)\right]$, $I_v(.)$ is the v-th order modified Bessel function of the first kind and $L_{1/2}(0) = 1$.

Now, $E[|H|^2]$ can be expressed as

$$\begin{aligned} E[|H|^2] &= (N^2-N)\frac{\pi^2}{4}\sigma_k^4\left[L_{1/2}\left(-\frac{v_k^2}{2\sigma_k^2}\right)\right]^4 \\ &\quad + N\left(2\sigma_k^2+v_k^2\right)^2 \\ &= (N^2-N)\frac{\pi^2}{4}\frac{1}{4}\left[L_{1/2}(0)\right]^4 \\ &\quad + N\left(2\frac{1}{2}+0\right)^2 \\ &= (N^2-N)\frac{\pi^2}{16} - N. \end{aligned} \tag{66}$$

The variance of H,i.e., $Var[|H|]$ can be expressed as

$$\begin{aligned} Var[|H|] &= N\left[2\sigma_k^2 - \frac{\pi^2}{4}\sigma_k^4\left\{L_{1/2}\left(-\frac{v_k^2}{2\sigma_k^2}\right)\right\}^4\right] \\ &\quad + Nv_k^2 \\ &= N\left[2\frac{1}{2} - \frac{\pi^2}{4}\frac{1}{4}\left\{L_{1/2}(0)\right\}^4\right] \\ &\quad + N(0) \\ &= N\left(1-\frac{\pi^2}{16}\right). \end{aligned} \tag{67}$$

(ii) **Dominant LoS:** When LoS is dominant, $v_k > \sigma_k^2$. To find the $E[|H|]$ and $Var[|H|]$, it is considered that $v_k = 1$ and $\sigma_k^2 = \frac{1}{4}$. Substituting the values of v_k and σ_k^2 in the expression of $E[|h_k|]$ and $Var[|h_k|]$, the mean values of h_k and g_k can be defined as $E[|h_k|] = E[|g_k|] = \frac{1}{2}\sqrt{\frac{\pi}{2}}L_{1/2}(-2)$ and $Var[|h_k|] = Var[|g_k|] = \frac{3}{2} - \frac{\pi}{8}\left[L_{1/2}(-2)\right]^2$, $L_{1/2}(-2) = 0.667$. Using the same process as done in (65) and (67), $E[|H|]$ and $Var[|H|]$ can be expressed as,

$$\begin{aligned} E[|H|] &= \frac{N\pi}{2}\sigma_k^2\left[L_{1/2}\left(-\frac{v_k^2}{2\sigma_k^2}\right)\right]^2 \\ &= \frac{N\pi}{2}\frac{1}{4}\left[L_{1/2}(-2)\right]^2 \\ &= \frac{0.445\,N\pi}{8}, \end{aligned} \tag{68}$$

where $L_{1/2}(-2) = 1.81$.

$$\begin{aligned} Var[|H|] &= N\left[2\sigma_k^2 - \frac{\pi^2}{4}\sigma_k^4\left\{L_{1/2}\left(-\frac{v_k^2}{2\sigma_k^2}\right)\right\}^4\right] \\ &\quad + Nv_k^2 \\ &= N\left[2\frac{1}{4} - \frac{\pi^2}{4}\frac{1}{16}\left\{L_{1/2}(-2)\right\}^4\right] \\ &\quad + N(1) \\ &= N\left(\frac{1}{2} - \frac{0.1979\pi^2}{64}\right) + N. \end{aligned} \tag{69}$$

APPENDIX B

$$\begin{aligned} Z &= \int_0^{\bar{\gamma}_{th1}} f_{H_{eq}}(x)dx \\ &= \frac{1}{b^{a+1}\Gamma(a+1)}\int_0^{\bar{\gamma}_{th1}} x^a exp\left(-\frac{x}{b}\right)dx, \end{aligned} \tag{70}$$

where $\bar{\gamma}_{th1} = \sqrt{\frac{\gamma_{th}}{C_1 - C_2\gamma_{th}}}$. Above integral is bounded by 0 to $\bar{\gamma}_{th1}$ can be replaced by $\left[\frac{a!}{(1/b)^{a+1}} - exp(-\bar{\gamma}_{th1})\sum_{k=0}^{a}\frac{a!\bar{\gamma}_{th1}^k}{k!(1/b)^{a-k+1}}\right]$ using [36, (3.35, page-340)].

$$\begin{aligned} Z &= \int_0^{\bar{\gamma}_{th1}} f_{H_{eq}}(x)dx \\ &= \frac{1}{b^{a+1}\Gamma(a+1)}\left[\frac{a!}{(1/b)^{a+1}}\right. \\ &\quad \left. -exp(-\bar{\gamma}_{th1})\sum_{k=0}^{a}\frac{a!\bar{\gamma}_{th1}^k}{k!(1/b)^{a-k+1}}\right]. \end{aligned} \tag{71}$$

After doing some algebra and using [36, (3.351.1, page-340)], (49) can be reduced to

$$Z = \frac{1}{b^{a+1}\Gamma(a+1)}(1/b)^{-a-1}\gamma\left(a+1, \frac{\bar{\gamma}_{th1}}{b}\right). \quad (72)$$

Similarly, the outage probability $P_{out,D2}$ can also be evaluated.

APPENDIX C

The PDF of H_i and H_j follow the distribution of H. Thus, $f_{H_i}(x)$ and $f_{H_j}(y)$ can be expressed as,

$$f_{H_i}(x) = \frac{1}{C_4}x^a exp\left(-\frac{x}{b}\right), \quad (73)$$

$$f_{H_i}(y) = \frac{1}{C_4}y^a exp\left(-\frac{y}{b}\right), \quad (74)$$

where $C_4 = \frac{1}{b^{a+1}\Gamma(a+1)}$.

$$H_{ij} = H_i + H_j, \quad (75)$$

where H_i and H_j are independent of each other. Hence the PDF of H_{ij} can be written as,

$$f_{H_{ij}}(z) = \int_0^\infty f_{H_i}(x)f_{H_j}(y)dx = \int_0^\infty f_{H_i}(x)f_{H_j}(z-x)dx. \quad (76)$$

After substituting $f_{H_i}(x)$ and $f_{H_j}(z-x)$ in (76), and after doing some algebra, (76) reduces to

$$f_{H_{ij}}(z) = \frac{exp(\frac{-z}{b})}{C_4^2}\int_0^\infty x^a(z-x)^a dx. \quad (77)$$

Since $a > 1$, (77) doesn't converge. To get a closed form of $f_{H_{ij}}(z)$, (77) modified to

$$f_{H_{ij}}(z) = \frac{exp(\frac{-z}{b})}{C_4^2}\int_0^z x^a(z-x)^a dx, \quad (78)$$

where $z \neq \infty$. After doing some algebra, using [36], and replacing C_4, (78) reduces to

$$f_{H_{ij}}(z) = \frac{exp\left(-\frac{z}{b}\right)}{\left[b^{a+1}\Gamma(a+1)\right]^2}z^{2a+1}B\left(a+1, a+1\right),$$

where $B(.,.)$ is the Beta function, $B(p,q) = \int_0^1 t^{p-1}(1-t)^{q-1}dt$, and z is a dummy variable.

APPENDIX D

$$\begin{aligned} P_{out,D1,C} &= P\left(\gamma_{D1,C} \leq \gamma_{th}\right) \\ &= P\left(H_{ij} \leq \bar{\gamma}_{th1}\right) \\ &= \int_0^{\bar{\gamma}_{th1}} f_{H_{ij}}(x)dx \\ &= \frac{B(a+1,a+1)}{[b^{a+1}\Gamma(a+1)]^2}\int_0^{\bar{\gamma}_{th1}} x^{2a+1}exp\left(-\frac{x}{b}\right)dx. \end{aligned} \quad (79)$$

After some algebraic manipulation and using [36, (3.191.1, page-315)], the expression of $P_{out,D1,C}$ can be reduced to

$$P_{out,D1,C} = \frac{B(a+1,a+1)}{[b^{a+1}\Gamma(a+1)]^2}(1/b)^{-2a-2}\gamma\left(2a+2, \frac{\bar{\gamma}_{th1}}{b}\right).$$

Similarly, the outage probability $P_{out,D2,C}$ can also be evaluated.

REFERENCES

[1] X. Liu, B. Xu, X. Wang, K. Zheng, K. Chi, and X. Tian, "Impacts of sensing energy and data availability on throughput of energy harvesting cognitive radio networks," *IEEE Trans. Veh. Technol.*, vol. 72, no. 1, pp. 747–759, Jan. 2023.

[2] R. I. Ansari, C. Chrysostomou, S. A. Hassan, M. Guizani, S. Mumtaz, J. Rodriguez, and J. J. P. C. Rodrigues, "5G D2D networks: Techniques, challenges, and future prospects," *IEEE Syst. J.*, vol. 12, no. 4, pp. 3970–3984, Dec. 2018.

[3] J. Wang, Z. Gong, and Y. Wei, "Multi-phase device-to-device relay algorithms for data dissemination in a cluster," in *Proc. 21st Int. Conf. Telecommun. (ICT)*, May 2014, pp. 201–205.

[4] M. Waqas, Y. Niu, Y. Li, M. Ahmed, D. Jin, S. Chen, and Z. Han, "A comprehensive survey on mobility-aware D2D communications: Principles, practice and challenges," *IEEE Commun. Surveys Tuts.*, vol. 22, no. 3, pp. 1863–1886, 3rd Quart., 2020.

[5] Q. Wu, S. Zhang, B. Zheng, C. You, and R. Zhang, "Intelligent reflecting surface-aided wireless communications: A tutorial," *IEEE Trans. Commun.*, vol. 69, no. 5, pp. 3313–3351, May 2021.

[6] E. Basar, "Reconfigurable intelligent surfaces for Doppler effect and multipath fading mitigation," *Frontiers Commun. Netw.*, vol. 2, pp. 1–17, May 2021. [Online]. Available: https://www.frontiersin.org/articles/10.3389/frcmn.2021.672857

[7] J. Huang, C.-X. Wang, Y. Sun, R. Feng, J. Huang, B. Guo, Z. Zhong, and T. J. Cui, "Reconfigurable intelligent surfaces: Channel characterization and modeling," *Proc. IEEE*, vol. 110, no. 9, pp. 1290–1311, Sep. 2022.

[8] S. Basharat, M. Khan, M. Iqbal, U. S. Hashmi, S. A. R. Zaidi, and I. Robertson, "Exploring reconfigurable intelligent surfaces for 6G: State-of-the-art and the road ahead," *IET Commun.*, vol. 16, no. 13, pp. 1458–1474, Aug. 2022. [Online]. Available: https://ietresearch.onlinelibrary.wiley.com/doi/abs/10.1049/cmu2.12364

[9] M. H. Khoshafa, T. M. N. Ngatched, and M. H. Ahmed, "Reconfigurable intelligent surfaces-aided physical layer security enhancement in D2D underlay communications," *IEEE Commun. Lett.*, vol. 25, no. 5, pp. 1443–1447, May 2021.

[10] Z. Peng, T. Li, C. Pan, H. Ren, and J. Wang, "RIS-aided D2D communications relying on statistical CSI with imperfect hardware," *IEEE Commun. Lett.*, vol. 26, no. 2, pp. 473–477, Feb. 2022.

[11] F. Yang, Y. Ni, W. Xia, Y. Liu, H. Zhang, and H. Zhao, "Ergodic achievable rate for RIS-assisted D2D communication over Nakagami-*m* fading," in *Proc. IEEE 22nd Int. Conf. Commun. Technol. (ICCT)*, Nov. 2022, pp. 1250–1254.

[12] A. K. Padhan, H. K. Sahu, P. R. Sahu, and S. R. Samantaray, "Performance analysis of smart grid wide area network with RIS assisted three hop system," *IEEE Trans. Signal Inf. Process. Over Netw.*, vol. 9, pp. 48–59, 2023.

[13] Y. Chen, B. Ai, H. Zhang, Y. Niu, L. Song, Z. Han, and H. V. Poor, "Reconfigurable intelligent surface assisted device-to-device communications," *IEEE Trans. Wireless Commun.*, vol. 20, no. 5, pp. 2792–2804, May 2021.

[14] S. W. H. Shah, A. N. Mian, S. Mumtaz, A. Al-Dulaimi, I. Chih-Lin, and J. Crowcroft, "Statistical QoS analysis of reconfigurable intelligent surface-assisted D2D communication," *IEEE Trans. Veh. Technol.*, vol. 71, no. 7, pp. 7343–7358, Jul. 2022.

[15] G. Wunder, P. Jung, M. Kasparick, T. Wild, F. Schaich, Y. Chen, S. T. Brink, I. Gaspar, N. Michailow, A. Festag, L. Mendes, N. Cassiau, D. Ktenas, M. Dryjanski, S. Pietrzyk, B. Eged, P. Vago, and F. Wiedmann, "5GNOW: Non-orthogonal, asynchronous waveforms for future mobile applications," *IEEE Commun. Mag.*, vol. 52, no. 2, pp. 97–105, Feb. 2014.

[16] Z. Ding, L. Lv, F. Fang, O. A. Dobre, G. K. Karagiannidis, N. Al-Dhahir, R. Schober, and H. V. Poor, "A state-of-the-art survey on reconfigurable intelligent surface-assisted non-orthogonal multiple access networks," *Proc. IEEE*, vol. 110, no. 9, pp. 1358–1379, Sep. 2022.

[17] T. Hou, Y. Liu, Z. Song, X. Sun, Y. Chen, and L. Hanzo, "Reconfigurable intelligent surface aided NOMA networks," *IEEE J. Sel. Areas Commun.*, vol. 38, no. 11, pp. 2575–2588, Nov. 2020.
[18] Z. Ding and H. Vincent Poor, "A simple design of IRS-NOMA transmission," *IEEE Commun. Lett.*, vol. 24, no. 5, pp. 1119–1123, May 2020.
[19] A. Hemanth, K. Umamaheswari, A. C. Pogaku, D.-T. Do, and B. M. Lee, "Outage performance analysis of reconfigurable intelligent surfaces-aided NOMA under presence of hardware impairment," *IEEE Access*, vol. 8, pp. 212156–212165, 2020.
[20] Y. Cheng, K. H. Li, Y. Liu, K. C. Teh, and H. Vincent Poor, "Downlink and uplink intelligent reflecting surface aided networks: NOMA and OMA," *IEEE Trans. Wireless Commun.*, vol. 20, no. 6, pp. 3988–4000, Jun. 2021.
[21] L. Yang and Y. Yuan, "Secrecy outage probability analysis for RIS-assisted NOMA systems," *Electron. Lett.*, vol. 56, no. 23, pp. 1254–1256, Nov. 2020.
[22] P. Kumar and A. Bhowmick, "Outage performance of reconfigurable intelligent surface assisted D2D network," in *Proc. IEEE 2nd Mysore Sub Sect. Int. Conf. (MysuruCon)*, Oct. 2022, pp. 1–5.
[23] M. H. N. Shaikh, S. Arzykulov, A. Celik, A. M. Eltawil, and G. Nauryzbayev, "Performance of RIS-empowered NOMA-based D2D communication under Nakagami-*m* fading," in *Proc. IEEE 96th Veh. Technol. Conf. (VTC-Fall)*, Sep. 2022, pp. 1–5.
[24] M. H. Kumar, S. Sharma, K. Deka, and M. Thottappan, "Reconfigurable intelligent surfaces assisted hybrid NOMA system," *IEEE Commun. Lett.*, vol. 27, no. 1, pp. 357–361, Jan. 2023.
[25] European Union. (Jan. 2021). *RISE-6G Project with a Horizon of 2030*. [Online]. Available: https://cordis.europa.eu/project/id/101017011/results
[26] E. C. Strinati, G. C. Alexandropoulos, V. Sciancalepore, M. Di Renzo, H. Wymeersch, D.-T. Phan-Huy, M. Crozzoli, R. D'Errico, E. De Carvalho, P. Popovski, P. Di Lorenzo, L. Bastianelli, M. Belouar, J. E. Mascolo, G. Gradoni, S. Phang, G. Lerosey, and B. Denis, "Wireless environment as a service enabled by reconfigurable intelligent surfaces: The RISE-6G perspective," in *Proc. Joint Eur. Conf. Netw. Commun. 6G Summit (EuCNC/6G Summit)*, Jun. 2021, pp. 562–567.
[27] L. Yang, Y. Yang, D. Benevides da Costa, and I. Trigui, "Outage probability and capacity scaling law of multiple RIS-aided networks," *IEEE Wireless Commun. Lett.*, vol. 10, no. 2, pp. 256–260, Feb. 2021.
[28] S. Jia, X. Yuan, and Y.-C. Liang, "Reconfigurable intelligent surfaces for energy efficiency in D2D communication network," *IEEE Wireless Commun. Lett.*, vol. 10, no. 3, pp. 683–687, Mar. 2021.
[29] L. Guo, J. Jia, Y. Zou, J. Chen, L. Yang, and X. Wang, "Resource allocation for multiple RISs assisted NOMA empowered D2D communication: A MAMP-DQN approach," *Ad Hoc Netw.*, vol. 146, Jul. 2023, Art. no. 103163. [Online]. Available: https://www.sciencedirect.com/science/article/pii/S1570870523000835
[30] Y. Wang, W. Zhang, Y. Chen, C.-X. Wang, and J. Sun, "Novel multiple RIS-assisted communications for 6G networks," *IEEE Commun. Lett.*, vol. 26, no. 6, pp. 1413–1417, Jun. 2022.
[31] G. C. Alexandropoulos, M. Crozzoli, D.-T. Phan-Huy, K. D. Katsanos, H. Wymeersch, P. Popovski, P. Ratajczak, Y. Bénédic, M.-H. Hamon, S. H. Gonzalez, R. D'Errico, and E. C. Strinati, "Smart wireless environments enabled by RISs: Deployment scenarios and two key challenges," in *Proc. Joint Eur. Conf. Netw. Commun. 6G Summit (EuCNC/6G Summit)*, Jun. 2022, pp. 1–6.
[32] B. C. Nguyen, L. T. Dung, T. M. Hoang, N. V. Vinh, and G. T. Luu, "On performance of multi-RIS assisted multi-user nonorthogonal multiple access system over Nakagami-*m* fading channels," *Comput. Commun.*, vol. 197, pp. 294–305, Jan. 2023. [Online]. Available: https://www.sciencedirect.com/science/article/pii/S0140366422004339
[33] J. Fang, C. Zhang, Q. Wu, and A. Li, "Improper Gaussian signaling for IRS assisted multiuser SWIPT systems with hardware impairments," *IEEE Trans. Veh. Technol.*, early access, May 8, 2023, doi: 10.1109/TVT.2023.3274365.
[34] C. Singh and C. Hsiang Lin, "Reconfigurable intelligent surfaces aided communication: Capacity and performance analysis over Rician fading channel," 2021, *arXiv:2107.10937*.
[35] G. Yang, X. Xu, and Y.-C. Liang, "Intelligent reflecting surface assisted non-orthogonal multiple access," in *Proc. IEEE Wireless Commun. Netw. Conf. (WCNC)*, May 2020, pp. 1–6.
[36] I. S. Gradshteyn and I. M. Ryzbik, *Table of Integrals, Series, and Products*. Academic, 2000.
[37] *Study on Downlink Multiuser Superposition Transmission for LTE*, document 36.859, 3rd Generation Partnership Project (3GPP), Valbonne, France, 2015.

PRADEEP KUMAR received the B.E. degree in electronics and telecommunication engineering from the Globus Engineering College, Madhya Pradesh, India, in 2007, and the M.S. degree in antenna and wave propagation from the Vellore Institute of Technology, Vellore, in 2015, where he is currently pursuing the Ph.D. degree. He was with the Koneru Lakshmaiah Educational Foundation (KLEF), Vijayawada, from 2017 to 2019. He has published research papers in several journals and conferences. His research interests include cognitive radio networks, with a focus on spectrum sensing and spectrum sharing issues, cooperative communications in cognitive radio networks, energy harvesting in wireless networks, D2D communication, and non-orthogonal multiple access (NOMA).

ABHIJIT BHOWMICK received the B.E. degree (Hons.) in electronics and telecommunication engineering from Burdwan University, West Bengal, India, in 2002, and the M.Tech. and Ph.D. degrees in telecommunication engineering from NIT Durgapur, in 2009 and 2016, respectively. He was with Cubix Control System Pvt. Ltd., from 2004 to 2006. He joined the Department of Electronics and Communication Engineering, Bengal College of Engineering and Technology, Durgapur, as a Lecturer, in 2006. He joined the School of Electronics Engineering (SENSE), Vellore Institute of Technology, Vellore, Tamil Nadu, India, in June 2016, where he is currently an Associate Professor. He has published more than 40 research papers in various journals and conferences. His research interests include cognitive radio networks, with a focus on spectrum sensing and spectrum sharing issues, cooperative communications in cognitive radio networks, energy harvesting in wireless networks, D2D communication, physical layer security issues in wireless networks, and UAV-assisted communication. He is a reviewer of several IEEE, Springer, Wiley, and Elsevier conferences and journals.

YOGESH KUMAR CHOUKIKER (Senior Member, IEEE) received the B.E. degree, in 2007, and the M.Tech. and Ph.D. degrees in electronics engineering from the National Institute of Technology, Rourkela, Orissa, India, in 2009 and 2014, respectively. He specialized in antenna and wave propagation. His research interests include microstrip antenna (fractal antennas) in the area of wireless applications, MIMO environment, UWB, and reconfigurable fractal. He was a Visiting Research Scholar with San Diego State University, San Diego, CA, USA, during the Ph.D. degree. Since January 2014, he has been a Professor with the Vellore Institute of Technology, Vellore. He completed the ISRO respond project, in 2013, which is based on optimization techniques. He has completed two SERB Government of India projects. He published more than 70 research papers in referred journals and international conferences/symposia. He is a Reviewer of the research paper for IEEE Transactions on Antennas and Propagation, IEEE Transactions on Microwave and Theory Techniques, IEEE Antennas and Wireless Propagation Letters, *International Journal of RF and Microwave Computer-Aided Engineering*, and *IET Microwave, Antennas, & Propagation*.